

Supplementary Information

High thermoelectric performance of BiCuSeO by optimized carrier concentration and point defect scattering through Cr-induced compositing effect

Asep Ridwan Nugraha,^{*a} Shamim Sk,^b Andrei Novitskii,^b Dedi,^d Fainan Failamani,^e
Bambang Prijamboedi,^e Takao Mori,^{b,c} and Agustinus Agung Nugroho^e

^a *Physics Graduate Program, Institut Teknologi Bandung, Jl. Ganesha 10, Bandung 40132, Indonesia.*

^b *Research Center for Materials Nanoarchitectonics (MANA), National Institute for Materials Science (NIMS), Namiki 1-1, Tsukuba 305-0044, Japan.*

^c *Graduate School of Pure and Applied Sciences, University of Tsukuba, Tennodai 1-1-1, Tsukuba 305-8573, Japan.*

^d *Research Center for Electronics, National Research and Innovation Agency (BRIN), Jl. Sangkuriang, Bandung 40135, Indonesia.*

^e *Faculty of Mathematics and Natural Sciences (FMIPA), Institut Teknologi Bandung (ITB), Jl. Ganesha 10, Bandung 40132, Indonesia.*

**Email: ase051@brin.go.id*

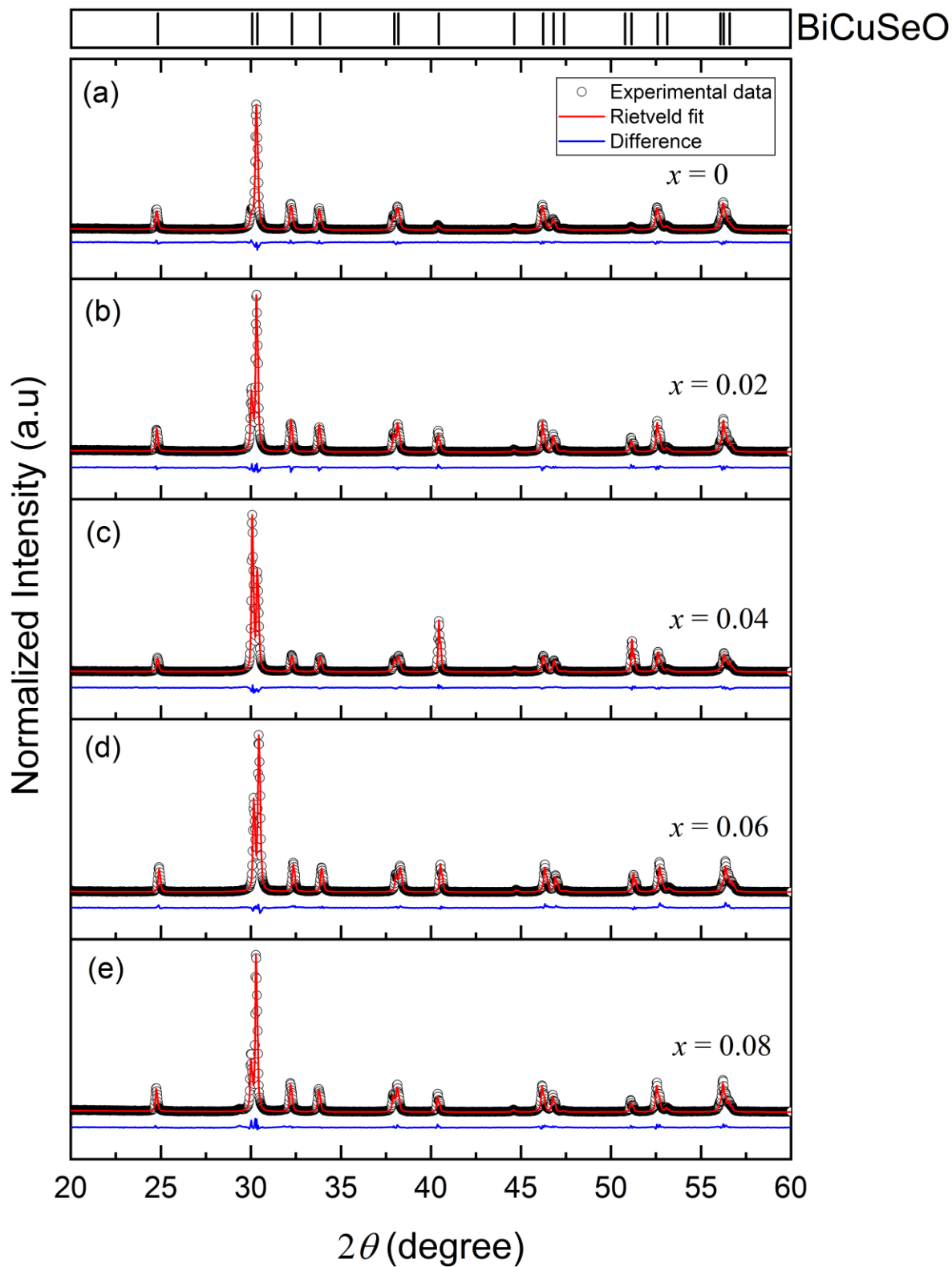


Figure S1. Rietveld refinement of powder XRD pattern for $\text{BiCu}_{1-x}\text{Cr}_x\text{SeO}$ ($x = 0, 0.02, 0.04, 0.06, 0.08$) with normalized observed intensity in circle symbol, Rietveld fit in red line, differences in blue line, and reference BiCuSeO as a black solid line at the top of the figure.

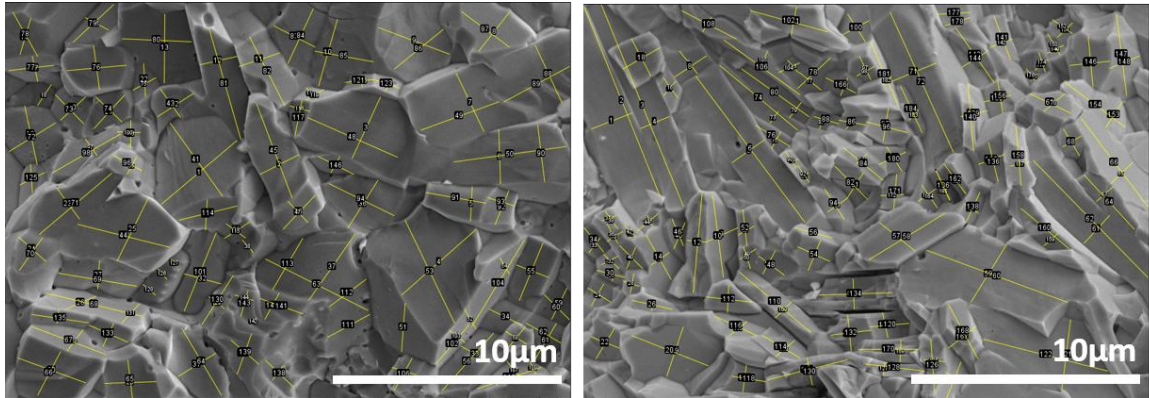


Figure S2. Calculated grind size from SEM images

- The average grain size of $\text{BiCu}_{1-x}\text{Cr}_x\text{SeO}$ for $x = 0$ and 0.04 are $2.1 \mu\text{m}$ and $1.8 \mu\text{m}$, respectively.
- The percentage of grains with size below $2 \mu\text{m}$ is 56%, 2-4 μm is 35%, and $>4 \mu\text{m}$ is 9% for Pristine BiCuSeO
- The percentage of grains with size below $2 \mu\text{m}$ is 69%, 2-4 μm is 23%, and $>4 \mu\text{m}$ is 8% for $x = 0.04$ sample.

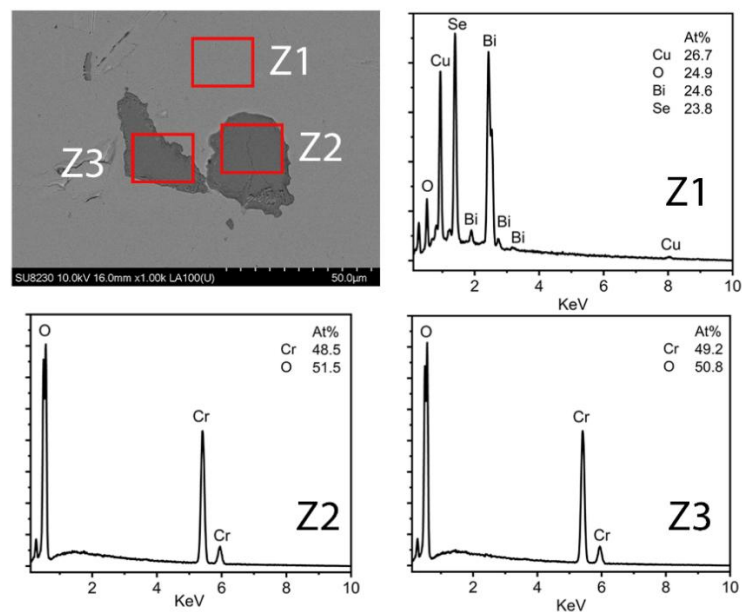


Figure S3. $\text{BiCu}_{0.96}\text{Cr}_{0.04}\text{SeO}$ with composition analysis of the Z1, Z2 and Z3

The SEM images of the polished $\text{BiCu}_{0.96}\text{Cr}_{0.04}\text{SeO}$ sample are shown in Fig. S3. The contrast between CrO secondary phase and the BiCuSeO matrix can be clearly seen. The EDS composition analysis was performed on the Z1, Z2 and Z3 regions. It can be seen that the polished area (Z2 & Z3) is obviously rich in Cr element compared to the matrix (Z1), further confirming the composite of CrO.

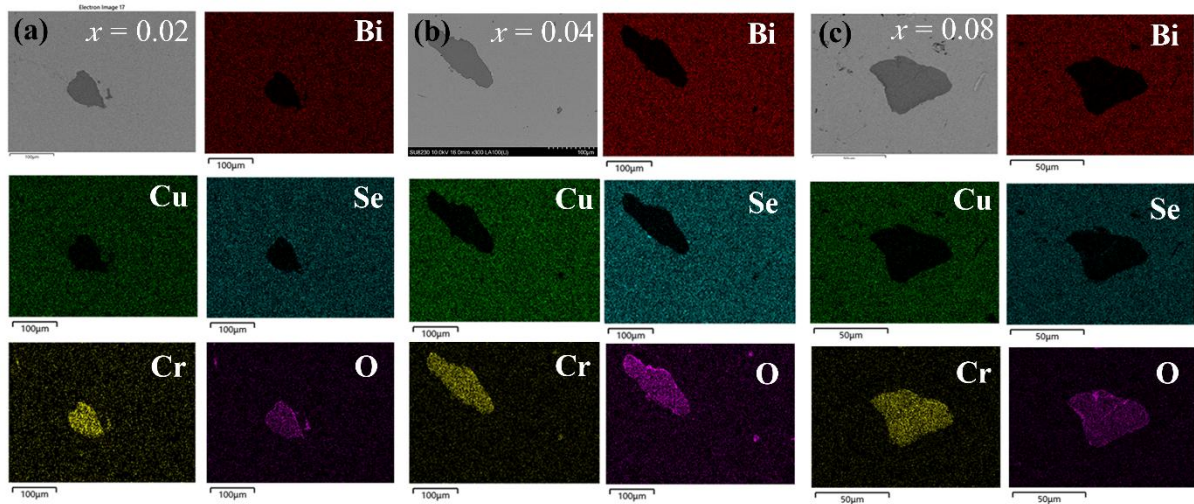


Figure S4. The elemental mapping of the Bi, Cu, Se, Cr and O atoms in the $\text{BiCu}_{1-x}\text{Cr}_x\text{SeO}$ samples with (a) $x = 0.02$, (b) $x = 0.04$, and (c) $x = 0.08$, respectively.

As can be seen in Figure S4, the Cr tends to form nano- to microscale precipitates of CrO, even at the lowest Cr concentration, indicating very low solubility of Cr in BiCuSeO matrix.

Reproducibility of the sample

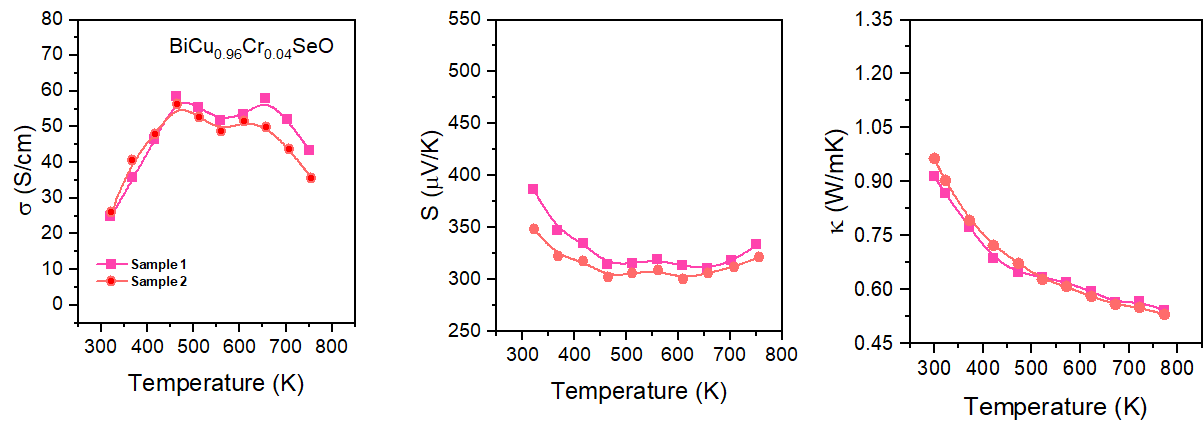


Figure S5. The reproducibility of $\text{BiCu}_{0.96}\text{Cr}_{0.04}\text{SeO}$ sample.

These samples (sample 1 and 2) of the $\text{BiCu}_{0.96}\text{Cr}_{0.04}\text{SeO}$ were synthesized using the same method and the results demonstrate good reproducibility among the samples.

Specific Heat Calculation & Thermal Diffusivity:

The temperature dependence of specific heat capacity is calculated using Debye model when $T > \theta_D$ with following equation

$$C_p = \gamma T + \frac{9Rn}{M} \cdot \left(\frac{T}{\theta_D}\right)^3 \cdot \int_0^{\theta_D/T} \frac{x^4 e^x}{(e^x - 1)^2} dx \quad (\text{S1})$$

where γ is the Sommerfeld coefficient, $\gamma = 3.075 \cdot 10^{-7} \text{ J g}^{-1} \text{ K}^{-2}$ [1], R is the ideal gas constant, n is the number of atoms, M is the molar mass, θ_D is the Debye temperature, $\theta_D = 243 \text{ K}$ [2], and $x = hv/k_B T$. The Debye temperature and the Sommerfeld coefficient were assumed to be independent of the doping level. According to eq. (S1), the calculated specific heat capacity of the $\text{BiCu}_{1-x}\text{Cr}_x\text{SeO}$ samples is slightly higher than pristine BiCuSeO due to the atomic mass difference between Cr (51.9961) and Cu (63.546) atoms. The thermal diffusivity is measured by laser flash method using LFA427, Netzsch, Germany. The typical dimension that used in thermal diffusivity measurement is 10 mm in diameter with a thickness of approximately ~ 1.7 mm.

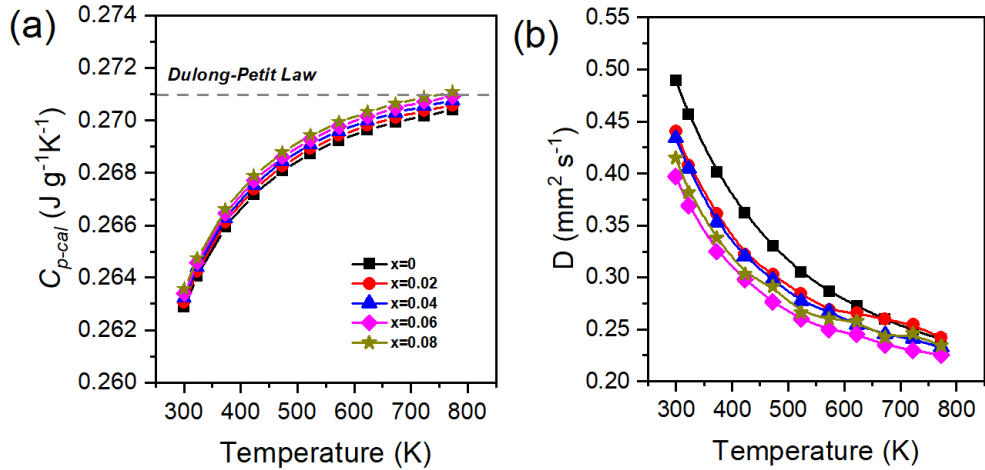


Figure S6. Thermal properties as a function of temperature of the $\text{BiCu}_{1-x}\text{Cr}_x\text{SeO}$ ($x = 0; 0.02; 0.04; 0.06; 0.08$) (a) specific heat capacity, (b) thermal diffusivity.

Lorenz number calculation & electronic thermal conductivity:

The total thermal conductivity (κ) is defined as a sum of the electronic (κ_e) and lattice thermal conductivity (κ_l). The electronic part κ_e is directly proportional to the electrical conductivity σ

through the Wiedemann-Franz relation, $\kappa_e = L\sigma T$, where L is the Lorenz number [3]. The Lorenz number depends on the scattering parameter (r) and will decrease as the reduced Fermi energy (η) decreases with increasing temperature. The Lorenz number can be given as: [4]

$$L = \left(\frac{k_B}{e}\right)^2 \left(\frac{(r+\frac{7}{2})F_{r+\frac{5}{2}}(\eta)}{(r+\frac{3}{2})F_{r+\frac{1}{2}}(\eta)} - \left[\frac{(r+\frac{5}{2})F_{r+\frac{3}{2}}(\eta)}{(r+\frac{3}{2})F_{r+\frac{1}{2}}(\eta)} \right]^2 \right) \quad (\text{S2})$$

For the Lorenz number calculation, we need to calculate the reduced Fermi energy (η) from the measured Seebeck coefficients compared to the calculated Seebeck coefficient by using the following relationship:

$$S = \pm \frac{k_B}{e} \left(\frac{(r+\frac{5}{2})F_{r+\frac{3}{2}}(\eta)}{(r+\frac{3}{2})F_{r+\frac{1}{2}}(\eta)} - \eta \right) \quad (\text{S3})$$

where $F_n(\eta)$ is the n -th order Fermi integral,

$$F_n(\eta) = \int_0^\infty \frac{\chi^n}{1+e^{\chi-\eta}} d\chi \quad (\text{S4})$$

$$\eta = \frac{E_f}{k_B T} \quad (\text{S5})$$

where, k_B , e , and E_f are the Boltzmann constant, the electron charge, and the Fermi energy. By assuming that the acoustic phonon scattering ($r = -1/2$) is the main scattering mechanism, the Lorenz number can be obtained by applying the calculated reduced Fermi energy η and scattering parameter r into Eq. (S2). Table S1 shows the calculated Lorenz number for pristine BiCuSeO as representative. Figs. S7 (a-b) show the Lorenz number and electronic thermal conductivity of the BiCu_{1-x}Cr_xSeO as a function of temperature.

Table S1. The Lorenz number for pristine BiCuSeO as a function of temperature

T (K)	S_{exp} (μVK^{-1})	$S_{(\text{SPB-APS})}$ (μVK^{-1})	η	L ($\text{W}\Omega\text{K}^{-2}$) $\times 10^{-8}$
306	497.97	497.97	-3.76	1.49
322	491.72	491.72	-3.69	1.49
369	488.65	488.65	-3.65	1.49
417	488.14	488.14	-3.64	1.49
464	484.55	484.55	-3.60	1.49
512	467.72	467.72	-3.40	1.50
561	446.42	446.42	-3.15	1.50
610	428.99	428.99	-2.95	1.50
659	418.81	418.81	-2.82	1.50
707	411.29	411.29	-2.73	1.50
756	404.34	404.34	-2.65	1.50

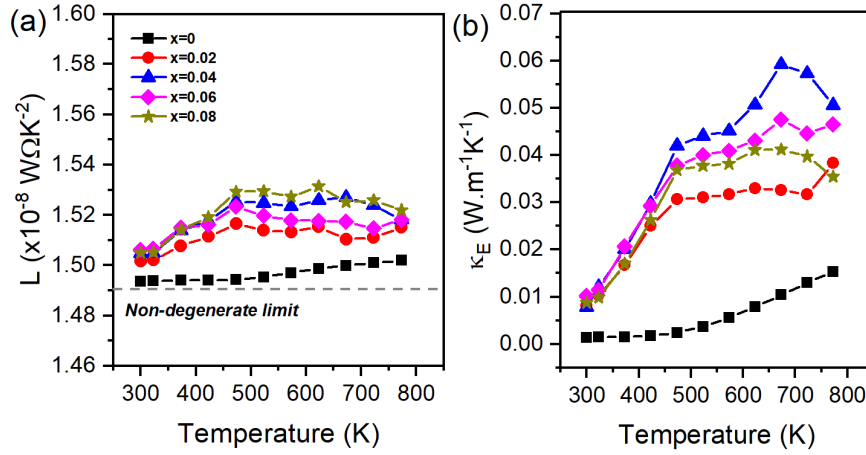


Figure S7. (a) Lorenz number, (b) electronic thermal conductivity of the $\text{BiCu}_{1-x}\text{Cr}_x\text{SeO}$ ($x = 0; 0.02; 0.04; 0.06; 0.08$) as a function of temperature.

Callaway model calculation:

In a solid solution system, point defects scattering originates from both the mass difference (mass fluctuations) and the size and the interatomic coupling force differences (strain field fluctuations) between the impurity atom and the host lattice. Callaway model has been applied to describe the influence of point defects on the lattice thermal conductivity [5–7]. We present a phonon scattering model based on the above theory and try to describe the effect of Cr addition on the lattice thermal conductivity of BiCuSeO system.

At temperature above the Debye temperature, the ratio of the lattice thermal conductivities of a material containing defects to that of the parent material can be written as: [5–7]

$$\frac{\kappa_L}{\kappa_{L,p}} = \frac{\tan^{-1}(u)}{u} \quad (\text{S6})$$

where κ_L , $\kappa_{L,p}$ are the lattice thermal conductivities of the defected and parent materials, respectively, and the parameter u is defined by:

$$u = \left(\frac{\pi^2 \theta_D \Omega}{h v_a^2} \kappa_{L,p} \Gamma \right)^{\frac{1}{2}} \quad (\text{S7})$$

where h , Ω , v_a and θ_D stand for the Planck constant, average volume per atom, lattice sound velocity, and the Debye temperature.

$$v_a = \left(\frac{1}{3} \left[\frac{1}{v_l^3} + \frac{2}{v_s^3} \right] \right)^{-\frac{1}{3}} \quad (\text{S8})$$

Here, the longitudinal (v_l , 3290m/s) and transverse (v_s , 1900m/s) sound velocities have been

obtained from previous research which gives v_a about 2107 m/s. Debye temperature θ_D is defined by: [8]

$$\theta_D = \frac{h}{k_B} \left[\frac{3N}{4\pi V} \right]^{\frac{1}{3}} v_a \quad (\text{S9})$$

where the V is the unit-cell volume, N is the number of atoms in a unit cell, k_B is Boltzmann parameter, and h presents the Planck constant. Eq. (S9) gives θ_D about 243 K.

The disorder scattering parameter (Γ) in eq. (S7) represents the strength of point defects phonon scattering, which includes two components, the scattering parameter due to mass fluctuations (Γ_M) and the scattering parameter due to strain field fluctuations (Γ_S) [9]. Often, the mass fluctuations (Γ_M) will be the dominant perturbation effect at a point defect, since the mass different from vacancy. The Klemens model using mass difference alone:

$$\Gamma = \Gamma_M \quad (\text{S10})$$

$$\Gamma_M = \frac{\langle \Delta M_n^2 \rangle}{\langle M \rangle^2} \quad (\text{S11})$$

Average mass of the compounds $\langle M \rangle$ is given by stoichiometry weighted average of each site average mass \overline{M}_n

$$\langle M \rangle = \frac{\sum_n c_n M_n}{\sum_n c_n} \quad (\text{S12})$$

The average mass for site 2 (Cu) in $\text{BiCu}_{1-x}\text{SeO}$ is

$$\overline{M}_2 = (1-x)M_{Cu} + xM_{vac} \quad (\text{S13})$$

if $M_{vac} = 0$, then $\overline{M}_2 = (1-x)M_{Cu}$

while the atomic mass averaged over the full solid is

$$\langle M \rangle = \frac{c_1 \overline{M}_1 + c_2 \overline{M}_2 + c_3 \overline{M}_3 + c_4 \overline{M}_4}{c_1 + c_2 + c_3 + c_4} = \frac{M_{Bi} + (1-x)M_{Cu} + M_{Se} + M_O}{4-x} \quad (\text{S14})$$

Average mass variance of the compound $\langle \Delta M^2 \rangle$ is given by stoichiometry weighted average of the all-mass variances $\overline{\Delta M_n^2}$

$$\langle \Delta M_n^2 \rangle = \frac{\sum_n c_n \overline{\Delta M_n^2}}{\sum_n c_n} \quad (\text{S15})$$

Where $\overline{\Delta M_n^2} = \sum_i f_{i,n} (M_{i,n} - \overline{M}_n)^2$

For example, atomic mass variance for site 2 (Cu) in $\text{BiCu}_{1-x}\text{SeO}$ is

$$\overline{\Delta M_2^2} = (1-x)(M_{Cu} - \overline{M}_2)^2 + x(M_{vac} - \overline{M}_2)^2 = (1-x)(M_{Cu} - \overline{M}_2)^2 + x(0 - \overline{M}_2)^2 \quad (\text{S16})$$

In vacancy scattering, a virial-theorem treatment for broken bonds suggests that the mass

difference on vacancy sites should be $M_{i,n} - \overline{M}_n = -M_{vac} - 2\langle \overline{M} \rangle$ as proposed by R. Gurunathan *et al.* [10]. However, in our system, tripling the mass difference of the vacancy could result in an overestimation of the disorder parameter. To ensure more precise calculations, we have adjusted the mass difference to be:

$$\overline{\Delta M_n^2} = \sum_i f_{i,n} (M_{i,n} - \overline{M}_n)^2 = (1-x)(M_{Cu} - \overline{M}_2)^2 + x(-M_{Cu} - 0.25\langle \overline{M} \rangle)^2 \quad (S17)$$

There is no change of the mass on the sites of Bi, Se and O, which gives:

$$\langle \Delta M_n^2 \rangle = \frac{\overline{\Delta M_n^2}}{4-x} \quad (S18)$$

Finally, the disorder parameter (Γ) can be calculated using equation S10-S18 as follow:

$$\Gamma_M = (4-x) \frac{(1-x)(M_{Cu} - \overline{M}_2)^2 + x(-M_{Cu} - 0.25\langle \overline{M} \rangle)^2}{(M_{Bi} + (1-x)M_{Cu} + M_{Se} + M_O)^2} \quad (S19)$$

After the calculation of point defects scattering on phonon for the disorder parameter (Γ) from those relative physical properties, we obtained perfect agreement between the calculated and measured values.

Table S2. The disorder parameters (Γ), measured κ_L , calculated κ_L and the difference between measured and calculated κ_L at room temperature.

x	$\Gamma (\times 10^{-2})$	κ_L (exp) ($\text{Wm}^{-1}\text{K}^{-1}$)	κ_L (calc) ($\text{Wm}^{-1}\text{K}^{-1}$)	diff (%)
0	0.000715	1.09	1.09	0.00365
0.02	1.43	0.97	1.02	5.15
0.04	2.87	0.95	0.97	2.11
0.06	4.31	0.89	0.92	3.37
0.08	5.74	0.91	0.88	3.30

The theoretical calculation of lattice thermal conductivity is performed according to the Debye – Callaway model [11].

$$\kappa_L = \frac{k_B}{2\pi^2 v_s} \left(\frac{k_B T}{h} \right)^3 \int_0^{\theta_D} \tau_{tot} \frac{x^4 e^x}{e^x - 1} dx \quad (S20)$$

where x is the reduced frequency ($x = \hbar\omega/k_B T$), ω the phonon angular frequency, k_B the Boltzmann constant, v_s the average sound speed, \hbar the reduced Planck constant, θ_D the Debye temperature, and τ_{tot} the combined phonon relaxation time. Assuming scattering channels are independent of each other, the τ_{tot} can be evaluated by Matthiessen's rule:

$$\tau_{tot}^{-1} = \tau_U^{-1} + \tau_{GB}^{-1} + \tau_{PD}^{-1} \quad (S21)$$

where τ_U , τ_{PD} , τ_{GB} are the relaxation time for Umklapp process (U), grain boundary scattering (GB) and point defect scattering (PD), respectively.

The relaxation time for point defect scattering is showed as follows: [11]

$$\frac{1}{\tau_{PD}} = A\omega^4; A = \frac{V_a}{4\pi v_s^3} \Gamma \quad (\text{S22})$$

where A is the fitting parameter, ω the phonon angular frequency, v_s is the average sound speed, V_a the atomic volume of the compound, Γ the disorder scattering parameter that characterizes the phonon scattering cross section of point defects. The disorder parameter (Γ) can be calculated by following equation S10 – S19 [12,13].

The relaxation time for Umklapp scattering at high temperature is [14]:

$$\frac{1}{\tau_U} = B\omega^2 T \quad (\text{S23})$$

where B is a fitting parameter, ω the phonon angular frequency, and θ_D the Debye temperature.

The relaxation time for the grain boundary scattering is:

$$\frac{1}{\tau_{GB}} = \frac{v_s}{d} \quad (\text{S24})$$

where v_s the average sound speed and d is the average grain size.

Since the value of B is not significantly changed by the Cr addition, the lattice thermal conductivity is found to depend on the value of A . The precise values of A and B were determined by fitting the equation S20-24 to the lattice thermal conductivity data. The resulting fitting parameter values for the calculated lattice thermal conductivity are presented in Table S3.

Table S3. Fitting parameters of calculated lattice thermal conductivity using Debye-Callaway model.

x	A ($\times 10^{-42} \text{ s}^3$)	B ($\times 10^{-17} \text{ sK}^{-1}$)
0	0.0013	2.9933
0.02	2.7458	3.1305
0.04	5.3899	3.1058
0.06	7.9316	3.0353
0.08	10.3702	3.0311

References:

- [1] C. Barreteau, D. Bérardan, E. Amzallag, L.D. Zhao, N. Dragoe, *Chemistry of Materials*, 2012, **24**, 3168–3178.
- [2] L. Pan, D. Bérardan, L. Zhao, C. Barreteau, N. Dragoe, *Appl Phys Lett*, 2013, **102**, 023902.
- [3] Fitsul, V. I. *Heavily Doped Semiconductors*; Plenum Press: New York, 1969.
- [4] Zhao, L.-D.; Lo, S.-H.; He, J. Q.; Li, H.; Biswas, K.; Androulakis, J.; Wu, C.-I.; Hogan, T. P.; Chung, D.-Y.; Dravid, V. P.; Kanatzidis, M. G. *J. Am. Chem. Soc.* **2011**, *133*, 20476.
- [5] Callaway, J.; Von Baeyer, H. C. *Phys. Rev.* 1960, **120**, 1149;
- [6] Dey, T. K.; Chaudhuri, K. D. *J. Low. Temp. Phys.* 1976, **23**, 419;
- [7] Yang, J.; Meisner, G. P.; Chen, L. *Appl. Phys. Lett.* 2004, **85**, 1140.
- [8] K. Kurosaki, A. Kosuga, H. Muta, M. Uno, S. Yamanaka, *Appl. Phys. Lett.* 2005, **87**, 061919.
- [9] C. L. Wan, W. Pan, Q. Xu, Y. X. Qin, J. D. Wang, Z. X. Qu, M. H. Fang, *Phys. Rev. B.* 2006, **74**, 144109.
- [10] Gurunathan, R.; *Phys. Rev. Appl.* 2020, **13** (3), 034011.
- [11] Callaway, J.; *Phys. Rev.* 1959, **113**, 1046–1051.
- [12] B. Abeles, *Phys. Rev.* 1963, **131**, 1906.
- [13] G. A. Slack, *Phys. Rev.* 1962, **126**, 427
- [14] P. G. Klemens, *Proc. Phys. Soc. Lond. A.* 1955, **68**, 1113-1128.